Transition Waves in Multi-stable Metamaterials with Space-time Modulated Potentials

Vinod Ramakrishnan[1] and Michael J. Frazier[1, a)]
Department of Mechanical and Aerospace Engineering, University of California, San Diego, California 92093, USA

This letter introduces a strategy for transition wave (soliton) management in multi-stable mechanical metamaterials, enabling on-demand, post-fabrication control of the associated phase transformation kinetics and distribution. Specifically, the wave dynamics are controlled by a small, kinematically-prescribed spatio-temporal variation in the elastic potential, constituting a driving force. The stability of the wave profile under slow-propagation conditions and the characteristic spatial localization of the Hamiltonian energy supports an analogy with a Newtonian particle traversing a viscous medium under forcing. The theoretical analysis adopts this particle perspective, describing the soliton dynamics through ordinary, rather than partial, differential equations. While myriad definitions for the potential modulation are possible, a traveling sinusoid assists the development of analytical solutions. Following this prescription, two wave propagation regimes are revealed: in one, the soliton is carried by the modulation with a commensurate velocity; in the other, the soliton is out-paced by the modulation and, thus, travels at reduced velocity. To illustrate the utility of this method, we demonstrate both the tractor and repulsor effects in multi-stable systems away from equilibrium: as a tractor (repulsor), the potential variation attracts (repels) the transition wave front in opposition to the system's energy-minimizing tendency. This method provides greater flexibility to the transformation performance of multi-stable metamaterials and supports the adoption of such systems in applications demanding multi-functionality.

Solitons[1] are a class of spatially localized, large-amplitude solutions to non-linear equations which describe a variety of processes within several domains of science, including biology[2–4], chemistry[5,6], cosmology[7,8], and the materials sciences[9–12]. In the context of materials with multiple equilibrium states, the propagation of topological solitons is a model for, e.g., polarization switching in ferroelectric[13] and ferromagnetic[14] materials, and structural phase transitions[15–17] – transformation phenomena which impact material performance and underpin multi-functionality in applications[18]. Recently, mechanical metamaterials[19] characterized by multi-stable internal architectures have exhibited similar behavior[20–28], extending atomic-scale physics and multi-functionality to the readily-accessible structural level. Command of the soliton dynamics promotes their utility in applications; however, for metamaterials, strategies for soliton management are few and often involve permanent modifications to the internal architecture (e.g., local/extended defects[24,26]) which "lock in" performance at fabrication, preventing on-demand control of the transformation kinetics and phase distribution. A means of soliton control which is amenable to post-fabrication adjustments is a desirable capability and motivates the present letter.

In practice, at the atomic scale, the environment in which a soliton [henceforth, synonymous with transition wave and (anti-)kink] propagates is hardly ideal: external fields, the effects of thermal noise, and structural impurities are each factors which affect the soliton dynamics and have been the subject of intense investigation, especially in the context of solid-state physics[29–31]. In addition to their relevance as incidental affects, these factors are simultaneously of practical import as instruments of transition wave control[32,33] which also extend to the metamaterial platform. In particular, the application of spatio-temporal forcing to the soliton wave front (e.g., by electric/magnetic fields) does not necessarily require permanent modifications to the internal architecture and opens the door to remote control. In the following, we study the dynamics of an elastic bi-stable lattice with spatio-temporal forcing arising from a similarly variable potential function; the modulation stimulating the propagation of otherwise static topological solitons with predictable velocity. The results contribute to the theoretical understanding of soliton dynamics in multi-stable metamaterials, facilitating the integration of these systems into applications demanding post-fabrication tuning and multi-functionality.

For the theoretical analysis, we consider the evolution of a one-dimensional, bi-stable continuous mechanical system, subject to prescribed spatio-temporal forcing, $f(x,t)$. The governing equation for the displacement field, $u(x,t)$, has the basic form

$$u_{,tt} - u_{,xx} + \psi'(u) = f(x,t) - \eta u_{,t}, \tag{1}$$

where η is the viscosity and $\psi'(u)$ is the force stemming from a symmetric, non-convex on-site potential, $\psi(u)$; one with two degenerate ground states, u_{S1} and u_{S2} (Fig. 1a). Under free-wave conditions ($\eta = 0, f = 0$), the system supports a number of traveling solutions; in particular, the topological modes (e.g., the anti-kink

a)Corresponding author email: mjfrazier@ucsd.edu

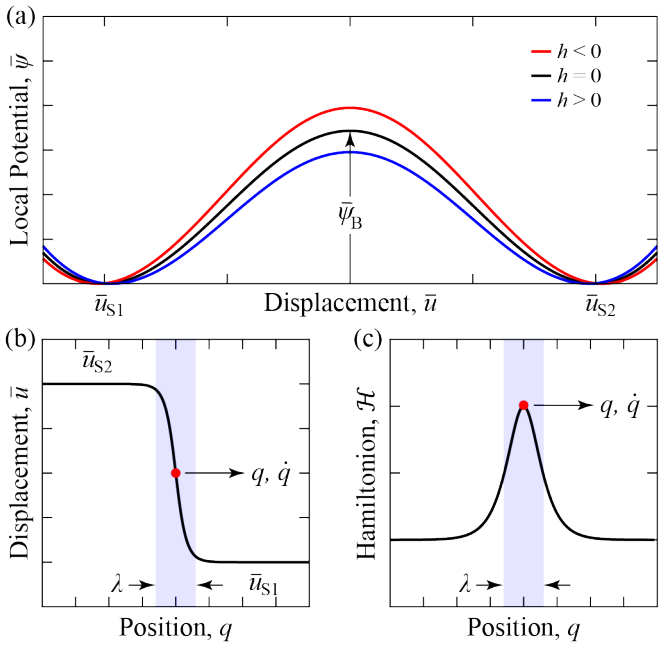

FIG. 1. Bi-stable Potential and Soliton Properties. (a) Local bi-stable potential facilitating the formation of (b) a soliton mode (anti-kink) with wavelength, λ, measuring the width of the transition region (shaded) [i.e., where $\psi''(u) < 0$]. The energy barrier, $\psi_{\mathbf{B}}$, separates degenerate ground states, u_{S1} and u_{S2}. (c) The Hamiltonian density, $\mathcal{H}$, exhibiting the characteristic soliton energy localization with $\mathcal{H} \to 0$ as $|q| \to \infty$. The dot identifies the energy maximum.

[Fig. 1b]) which we intend to manipulate. With characteristic length, a, a snapshot of the corresponding Hamiltonian density[34], $\mathcal{H} = \frac{1}{a}[\frac{1}{2}u_{,t}^2 + \frac{1}{2}u_{,x}^2 + \psi(u)]$, reveals the compact nature of the soliton energy distribution, reminiscent of a particle, an object with localized properties (Fig. 1c). Apart from myriad alternative choices, the point at which the energy density is maximal is a natural choice for the soliton center; therefore, for the soliton quasi-particle, we define the time-dependent position, $q(t) = (\Delta u)^{-1}\int_{-\infty}^{\infty} x u_{,x}\,\mathrm{d}x$, and velocity, $\dot{q}(t) = s(t) = (\Delta u)^{-1}\int_{-\infty}^{\infty} x u_{,xt}\,\mathrm{d}x$, where $\Delta u = \int_{-\infty}^{\infty} u_{,x}\,\mathrm{d}x$.

From $\mathcal{H}$, the total energy, E, of the free soliton particle is readily determined[34]:

$$E = \int_{-\infty}^{\infty} \mathcal{H}\mathrm{d}x = \sqrt{\frac{2}{1-s^2}}\int_{u_1}^{u_2} \sqrt{\psi(u)}\mathrm{d}u = m_0\gamma,$$

where $m_0 = \sqrt{2}\int\sqrt{\psi(u)}\mathrm{d}u$ is the particle rest mass. The relativistic mass, $m = m_0\gamma$, is tied to the soliton velocity, s, via the Lorentz contraction factor, $\gamma^{-1} = \sqrt{1-s^2}$. Likewise, γ also regulates the soliton shape, decreasing the wave width, λ, with increasing propagation speed. Thus, the mass properties of the proposed soliton particle are not fixed quantities. However, if $s \ll 1$ (i.e., $\gamma \approx 1$), then measures of the relativistic and rest mass coalesce, and the soliton profile is, essentially, unchanged compared to the static case. Provided that the slow propagation condition, $s \ll 1$, is realized, then the interpretation of the free soliton as a non-relativistic (i.e., Newtonian) particle is justified[34,35]; similarly, Eq. (1) represents a particle acted upon by perturbing forces, $-\eta u_{,t}$ and $f(x,t)$. In the following, we utilize the particle description to apply Newtonian dynamics to determine the response of transition waves to simultaneous space- and time-dependent forcing stemming from a similar dependency in the potential of the host medium. As a phenomenological construction, Eq. (2) is, perhaps, the simplest description of a dissipative system with independent local and non-local potential variation:

$$u_{,tt} - [1 + g(x,t)]\,u_{,xx} + [1 - h(x,t)]\,\psi'(u) = -\eta u_{,t}, \quad (2)$$

which can be arranged in the form of Eq. (1) with $f(x,t) = g(x,t)u_{,xx} + h(x,t)\psi'(u)$. More complicated formulations may, e.g., include additional spatial derivatives of u with space-time coefficients. In the context of the physical metamaterial, space-time coefficients such as $g(x,t)$ and $h(x,t)$ may be the effects of, e.g., prescribed external fields on stimuli-responsive elastic constituents or kinematically-activated geometric non-linearities.

Accompanying the particle position and velocity is the momentum, $p(t) = m\dot{q}(t)$, whose time rate-of-change balances the perturbing forces (see Supplemental Information [SI]):

$$\begin{aligned}\dot{p} &= \int_{-\infty}^{\infty} [f(x,t) - \eta u_{,t}]\,u_{,x}\,\mathrm{d}x \\ &= \int_{-\infty}^{\infty} f(x,t)u_{,x}\,\mathrm{d}x - \eta m\dot{q}(t) = m_0\gamma^3\ddot{q}(t),\end{aligned}$$

where we utilize the relation $p(t) = \int_{-\infty}^{\infty} u_{,t}\,u_{,x}\,\mathrm{d}x$. Evaluating the integral, $I(t) = \int_{-\infty}^{\infty} f(x,t)u_{,x}\,\mathrm{d}x$, and solving for $\ddot{q}(t)$ yields

$$\ddot{q}(t) = \frac{1}{m_0\gamma^3}I(t) - \frac{\eta}{\gamma^2}\dot{q}(t) \approx \frac{1}{m_0}I(t) - \eta\dot{q}(t), \quad (3)$$

the main theoretical result; the approximation recognizes the requisite slow-propagation condition, $s \ll 1$ (i.e., $\gamma \approx 1$). Furthermore, although soliton propagation may be stimulated by $f(x,t)$, if significant deformation of the soliton profile occurs, then the accuracy of the prediction [Eq. (3)] diminishes. Naturally, integrating Eq. (3) delivers the desired $q(t)$ and $\dot{q}(t)$.

To demonstrate the effectiveness of our strategy as well as to validate our theoretical predictions, we consider the non-linear dynamics of the discrete bi-stable metamaterial chain depicted in Fig. 2 which is a variant of the well-known system found in many theoretical[36–38] and experimental[22,24] studies. Although we could proceed with model stimuli-responsive stiffness elements (results are qualitatively similar [see SI]), we opt for a purely kinematic approach. The essential bi-stable element comprises two identical, pin-connected

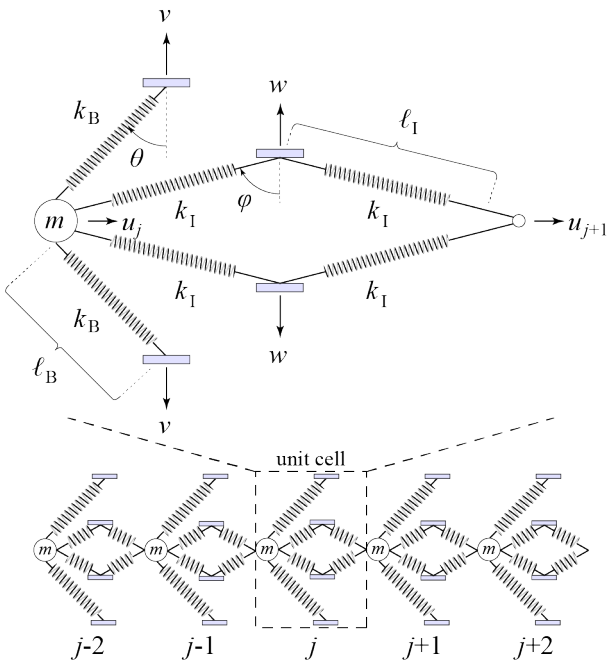

FIG. 2. Lattice with Space-Time Variable Potential. Prescribed displacements, $v(x,t)$ and $w(x,t)$ adjust the metamaterial geometry, facilitating local and non-local potential modulation, respectively.

springs of stiffness k_B symmetrically arranged about the horizontal axis. The mass, m, affixed to the common node is restricted to horizontal displacements, $\bar{u} = u/(\ell_B \sin\theta)$. Consequently, the corresponding on-site potential function, possesses two degenerate ground states $\bar{u}_{S1,S2} = 0, 2$. As one notable distinction with similar designs in prior studies, the remote ends of each spring may displace vertically, $\bar{v} = v/(\ell_B \cos\theta)$. As a second distinction, neighboring degrees of freedom, $\bar{u}_j$ and $\bar{u}_{j+1}$, are linked by spring assemblies which permit adjustments to the coupling strength through vertical displacements, $\bar{w} = w/(\ell_I \cos\varphi)$. For a lattice in which the vertical displacements depend on space and time, so too does the potential. In particular, $\bar{v}$ comprises a function which modifies the on-site potential in a manner similar to h in Fig. 1a. Thus, the non-dimensional equation of motion for an arbitrary degree of freedom, $\bar{u}_j$, within the lattice is (see SI)

$$\bar{u}_{j,\bar{t}\bar{t}} + \bar{\eta}\bar{u}_{j,\bar{t}} + \bar{\chi}_{,\bar{u}_j}(\bar{u}_j, \bar{u}_{j+1}) + \bar{\chi}_{,\bar{u}_j}(\bar{u}_j, \bar{u}_{j-1}) + [1 - h(\bar{u}_j, \bar{v}_j)]\,\bar{\psi}'(\bar{u}_j) = 0, \quad (4)$$

where $\bar{\chi}(\bar{u}_j, \bar{u}_{j\pm1})$ is the interaction potential function. The continuum approximation of the lattice governing equations resembles the form of Eq. (2). In simulation, we adopt the dimensionless material and geometric parameters $\bar{k}_B = 0.02$, $\bar{k}_I = 0.6728$, $\theta = \pi/4$, and $\varphi = \tan^{-1}(5/2)$. The system parameter, $\tau = 0.1$s, relates the dimensional and dimensionless times, $t = \tau\bar{t}$. The displacement amplitudes for $\bar{v}$ and $\bar{w}$ should be kept small in order to preserve the soliton profile consistent with the particle perspective ingrained in the theoretical results.

Figure 3 compares the predicted and simulated response of an initially static topological mode to a spatially prescribed on-site potential for various damping intensities. For the case in which the $\bar{v}_j$ change linearly (modulation in $\bar{w}$ yields qualitatively similar results [see SI]) such as to likewise lower the potential in the propagation direction (in this study, $\bar{\psi}_B$ is reduced, at most, by 2.5%), the simulated position and velocity are well-described by Eq. (3) as evidenced by the comparisons in Fig. 3a. The (anti-)kink travels down the potential grading the length of the lattice such that the associated phase transformation is uni-directional and complete. Nevertheless, since the bi-stable potential possesses degenerate ground states, the system supports both kink and anti-kink modes, facilitating reversible transformations[24]. Conceivably, e.g., following a binary scheme with $\bar{u}_{S1} \equiv$ ON and $\bar{u}_{S2} \equiv$ OFF, alternating soliton modes may constitute

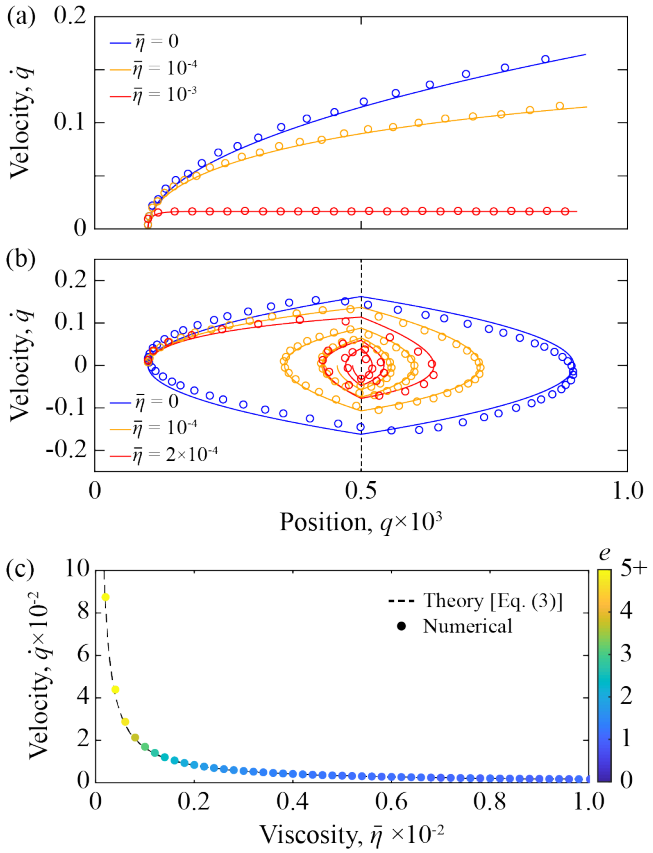

FIG. 3. (color online). Soliton in Static Potential Grading. A comparison of theoretically predicted (solid line) and numerically observed (dots) soliton response in (a) a linear and (b) a triangular potential grading (system minimum at $q = 500$) at various levels of material damping. (c) Percent error, e, in the numerical steady-state velocity results for a linear potential grading relative to that predicted by Eq. (3) as a function of damping intensity.

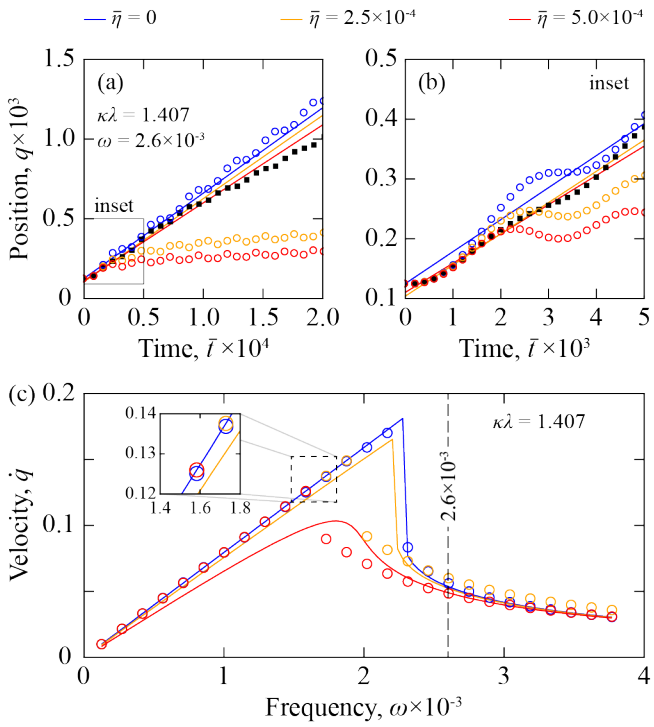

FIG. 4. Lattices with Space-Time Variable Potential. (a,b) A comparison of theoretically predicted (solid line) and numerically determined soliton position for a continuous sinusoidal modulation, $\bar{v}_j = \bar{V}\sin(\kappa ja + \vartheta - \omega\bar{t})$ (dots), and a pulsed sinusoidal modulation, $\bar{v}_j = \bar{V}\sin(\kappa ja + \vartheta - \omega\bar{t})\mathcal{H}(\mathrm{sgn}[\sin(\omega_s\bar{t})])$ (squares), with $\bar{V} = 2.5\times10^{-3}$ and $\omega_s = 2.1\times10^{-3}$. Different damping levels are represented for the continuous sinusoid. Only $\bar{\eta} = 5\times10^{-4}$ is plotted for the pulsed sinusoid. (c) A comparison of theoretically predicted (solid line) and numerically observed (dots) soliton velocities. The numerical velocities are calculated as the average velocity over a period, $T = 2\pi/\omega_r$.

damping-tolerant, continuous mechanical signals for information transmission in, e.g., completely soft robots and machines[39–41].

For vanishing initial conditions and non-zero viscosity, Eq. (3) gives $\dot{q}(\bar{t}) = I(1-\mathrm{e}^{-\bar{\eta}\bar{t}})/m_0\bar{\eta}$ as the soliton velocity which converges to the steady-state value $\dot{q}_{ss} = I/m_0\bar{\eta}$, a result similar to that obtained by Hwang and Arrieta[24] via a perturbation approach. Figure 3c compares the theoretical and numerical [at $\bar{t} \geq -\frac{1}{\bar{\eta}}\ln(0.01)$] results for $\dot{q}_{ss}$ as a function of the viscosity, revealing greater agreement toward higher values of $\bar{\eta}$ (equiv., slower propagation speeds) as measured by the relative percentage error, e. As $\bar{\eta}\to 0$ and the steady-state velocity increases, the relativistic effects disregarded in the formulation of Eq. (3) become significant, widening the discrepancy between theory and simulation.

For the case in which the $\bar{v}_j$ change non-monotonically, the traveling soliton may be trapped within a system-level local minimum. The trapped soliton oscillates about the minimum with a frequency determinable by Eq. (3) (see SI), causing the region to undergo repeated, autonomous transformations. Fig. 3b illustrates the oscillation of the soliton center in a (symmetric) system-level, triangular potential well. Naturally, dissipation alters the oscillation frequency and amplitude over time. Ultimately, the damped soliton settles into the minimum.

As a practical limitation, monotonic potential gradings prevent the construction of arbitrarily long lattices as the potential, ultimately, vanishes. However, a prescribed spatio-temporal variation in the potential manifesting mobile system-level minima may transport a transition wave front with a predictable velocity in lattices of any length.

We consider the response of an initially static transition wave in the proposed lattice where the prescribed displacement modulation, $\bar{v}_j = \bar{V}\sin(\kappa ja + \vartheta - \omega\bar{t})$, is a small-amplitude ($\bar{V} = 2.5\times10^{-3}$) sinusoid of frequency, ω, and wavenumber, κ. Consequently, the lattice possesses multiple potential minima which propagate with velocity $s_p = \omega/\kappa$ and to which the soliton is drawn, stimulating mobility. In the simulations, one of these minima is initially aligned with the soliton center at $q(0) = q_0$ using the phase shift, ϑ.

Figures 4a,b display the simulated soliton response to a continuous sinusoidal modulation for different damping intensities. In each case, the response (dots) exhibits an oscillatory behavior; however, while the undamped soliton propagates with a constant mean velocity, the damped soliton slows to a near halt, seemingly limiting the utility of the proposed strategy in practical (dissipative) systems. However, alternative modulation waveforms may be more effective in driving the damped soliton. For example, utilizing the pulsed sinusoid, $\bar{v}_j = \bar{V}\sin(\kappa ja + \vartheta - \omega\bar{t})\mathcal{H}(\mathrm{sgn}[\sin(\omega_s\bar{t})])$ ($\mathcal{H}$ is the Heaviside function), enables long propagation times even at $\bar{\eta} = 5\times10^{-4}$, a damping intensity which shortened propagation times in the case of the continuous sinusoid. Nevertheless, if the complexity of the modulation is measured by the number of tuning parameters in its mathematical description, then the continuous sinusoid is one of the simplest, and so, to simplify the theoretical analysis and exhibition of spatio-temporal potentials, the continuous sinusoid is applied in the following.

The governing equation corresponding to the sinusoidal modulation is (see SI)

$$\ddot{q}(\bar{t}) = \frac{I}{m_0}\cos(\vartheta - \omega_r\bar{t}) - \eta\dot{q}(\bar{t}), \tag{5}$$

where $\omega_r = \omega - \kappa\dot{q}$ and, for simplicity, we let $q_0 = 0$. To facilitate an analytical result from integration, we assume ω_r to be, essentially, constant which is approached in the case of small accelerations and times. Integrating Eq. (5)

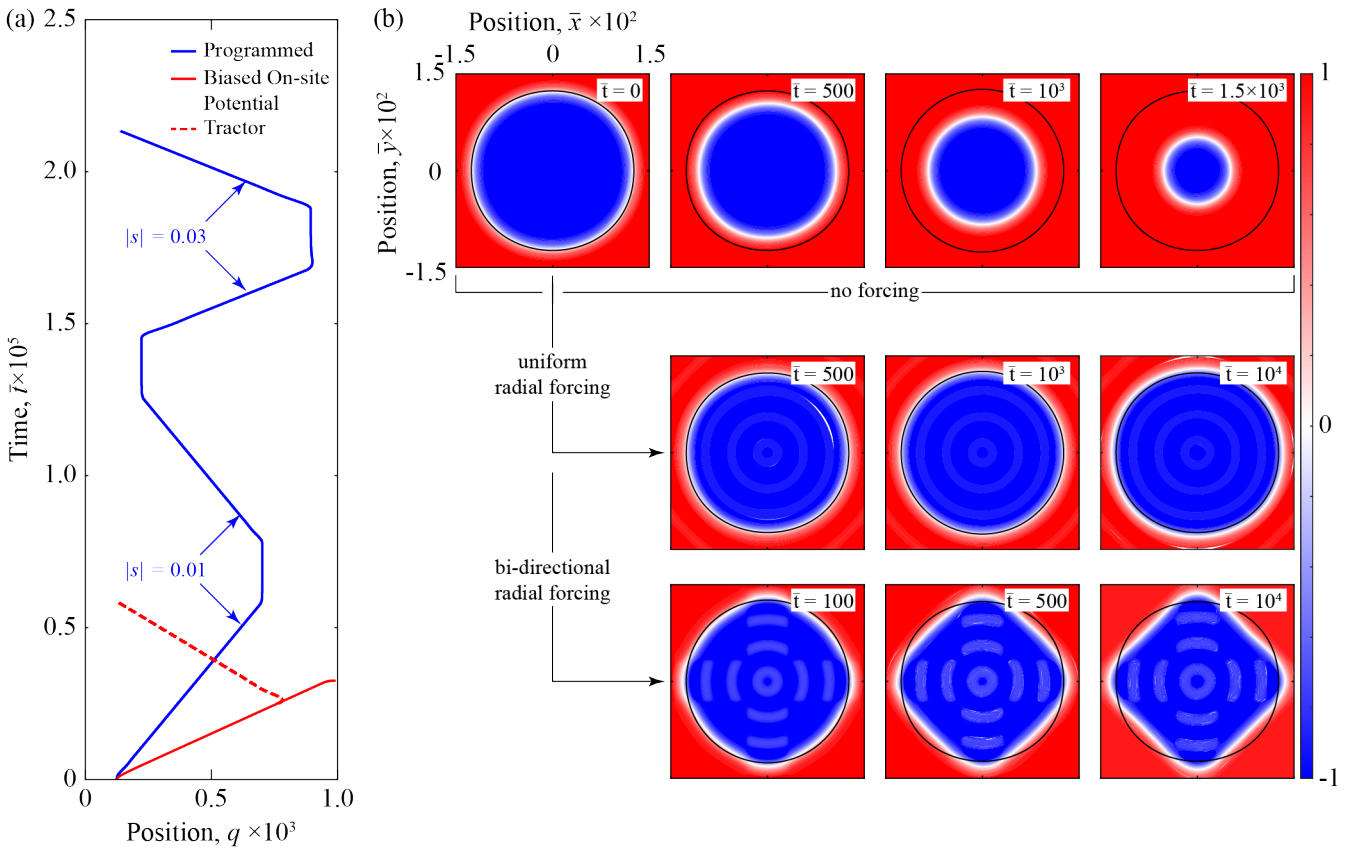

FIG. 5. Application of Spatio-Temporal Potential Modulation. (a) Soliton response to a programmed modulation and tractor beam ($\bar{V} = 0.0025$) (b) (top row) The collapse of a circular wave front in a 2D lattice in the absence of a potential variation; the expansion (middle row) and shaping (bottom row) of the same initial wave front due to a uniform radial ($\bar{V} = 0.0125$) and directional radial spatio-temporal variation ($\bar{V} = 0.05$) representing a repulsor.

yields

$$\dot{q}(\bar{t}) = s(\bar{t}) = \left[\frac{I}{m_0(\bar{\eta}^2+\omega_r^2)}\right] \left(\omega_r\left[\sin(\vartheta)e^{-\bar{\eta}\bar{t}} - \sin(\vartheta-\omega_r\bar{t})\right] - \bar{\eta}\left[\cos(\vartheta)e^{-\bar{\eta}\bar{t}} - \cos(\vartheta-\omega_r\bar{t})\right]\right).$$

Consistent with the small times assumption, we further consider $e^{-\bar{\eta}\bar{t}} \approx 1$ for several time periods, $T = 2\pi/\omega_r$, then the oscillatory behavior predicted by the above relation can be averaged over T to formulate the following cubic equation for the (perhaps transient) soliton mean speed over small times:

$$s^3 - 2s_p s^2 + \left[s_p^2 + \frac{\bar{\eta}^2}{\kappa^2} + \frac{I}{m_0\kappa}\sin(\vartheta)\right]s - \frac{I}{m_0\kappa^2}[\kappa s_p \sin(\vartheta) - \bar{\eta}\cos(\vartheta)] = 0. \quad (6)$$

For sufficiently slow moving modulations, the above polynomial possesses only one real root, $s \leq s_p$. Conversely, if the potential modulation travels with sufficient speed, there exists three real roots, the smallest of which is observed in simulations. These roots are plotted as solid lines in Figs. 4a,b, showing good agreement with the initial transient regions of the simulations, especially in the case $\bar{\eta} = 0$ for which $e^{-\bar{\eta}\bar{t}} = 1\ \forall\bar{t}$ and s may be interpreted as either the steady-state mean speed or, paradoxically, as the speed over a "transient" period of infinite duration. For the special case of $\bar{\eta} = 0$, the theoretical velocity is the piecewise expression

$$\dot{q} = \begin{cases} s_p, & s_p \leq s_c \\ \frac{1}{2}\left(s_p - \sqrt{s_p^2 - s_c^2}\right), & s_p > s_c \end{cases} \quad (7)$$

where the critical speed $s_c = \sqrt{4I\sin(\vartheta)/m_0\kappa}$ separates two kinetic regimes. For $s_p \leq s_c$, the speed of the potential modulation is sufficiently slow as to ensure that, as the minimum moves away from the soliton center, the transition wave is able to continuously re-equilibrate and, thus, travel with an identical mean, steady-state velocity, $\dot{q} = s_p$. Alternatively, in the region $s_p > s_c$, the soliton center is outpaced by the minima and, therefore, the transition wave travels at a reduced mean speed, alternately entering and exiting successive lattice-level potential wells. The damped soliton exhibits

qualitatively similar behavior, interestingly, leading to faster than predicted propagation for slow moving modulations. These results can be seen in Fig. 4c which compares ω-dependent theoretical and numerical results for different damping intensities, exhibiting excellent agreement, especially in the undamped scenario.

In the preceding, we theoretically describe and numerically analyze the physics of solitons in multi-stable metamaterials subject to spatio-temporal forcing, the result of a commensurate modulation in the elastic potential. In the context of soliton management, such an approach allows for the on-demand control of the kinetics and extent of phase transformations in systems of arbitrary size. To illustrate this ability, in the following, we present three examples of transition wave control. In each case, the spatio-temporal variation in the (on-site) potential stems from prescribed sinusoidal displacements, $\bar{v}_j = \bar{V}\sin(\kappa j a + \vartheta - \omega\bar{t})$.

For the moment, we consider a dissipative ($\bar{\eta} = 10^{-3}$) 1D metamaterial identical to that in Fig. 2 with the exception of an additional elastic component, $\bar{k}_{\mathrm{X}}$, which contributes $\bar{k}_{\mathrm{X}}\bar{u}^2/2$ to the on-site potential. In one scenario, $\bar{k}_{\mathrm{X}} = 0$, yielding degenerate ground states which prohibit the self-sustained propagation of transition waves[21,22]. Despite this condition, as shown in Fig. 5a, the movements of the soliton center may be programmed by utilizing a potential variation wherein κ and ω are assigned different values for specific time intervals: the soliton either remains static or propagates, including reversing propagation direction and altering propagation speed. In this manner, the kinetics and extent (i.e., position) of the associated phase transformation are controlled. In a second scenario, $\bar{k}_{\mathrm{X}} = 10^{-6}$ manifests a biased on-site energy landscape which supports the self-sustained, uni-directional propagation of a single soliton mode[24], rendering the corresponding transformation irreversible. Figure 5a plots the position of a transition wave front within the biased system, showing it to move with constant velocity until terminating at the system boundary at $q = 10^3$. However, while in transit, a spontaneous forcing – arbitrarily, initiated at $\bar{t} = 25\times10^3$ – stemming from a spatio-temporal potential variation counters the local energy bias and permits the reversal of the soliton propagation direction and, thus, the phase transformation in opposition to the energy minimizing tendency of the unforced system. In this manner, the modulation represents as a tractor.

For the third scenario, we consider a 2D bi-stable mechanical metamaterial modeled after that introduced in Frazier and Kochmann[23] (see SI) which possesses two degenerate ground states. Within this system, we initiate a circular phase which, subsequently, tends to collapse inward and vanish due to an energy-minimizing, "surface tension" effect related to the wave-front curvature. The snapshots in the first row of Fig. 5b depict this process. However, as indicated in the second row of Fig. 5b by the slight increase in the circular phase diameter, a radially directed spatio-temporal potential modulation is able to maintain the circular phase by repelling the wave front. Moreover, as illustrated in the third row, by directing the sinusoidal modulation along specific axes, the shape of the wave front can be deformed away from circular on demand. In opposing the natural tendency of the circular phase to collapse, the modulation acts as a repulsor.

In summary, this letter interprets (topological) solitons as Newtonian particles and applies the associated dynamics concepts to their prediction and control in multi-stable metamaterials. It was shown that spatio-temporal modulations of the metamaterial elastic potential stimulates soliton motion in a manner similar to the electric/magnetic fields in solid state systems. This represents means to manipulate the post-fabrication metamaterial phase transformation kinetics and phase distribution on demand and, potentially, remotely; a capability which supports the adoption of multi-stable metamaterials in applications demanding multi-functionality. The theoretical findings are supported by the simulation results of a representative metamaterial. Nevertheless, the particle interpretation restricts the forcing in order to avoid relativistic effects. In addition, without a check-and-amend scheme, the accuracy of theoretical predictions may diminish in time, especially when potentials possess a high degree of spatial variability, resulting in distortion of the soliton profile.

See supplementary material for animations, details of equation derivations and additional results for solitons in a potential grading induced by variation in w.

This work is supported by start-up funds provided by the University of California.

DATA AVAILABILITY

The data that supports the findings of this study are available within the article and its supplementary material.

[1] M. Remoissenet, *Waves called solitons: concepts and experiments*. Springer Science & Business Media, 2013.

[2] M. Peyrard, *Nonlinear Excitations in Biomolecules*. Springer, 1995. ISBN: 978-3-540-59250-1.

[3] J. Berry, C. P. Brangwynne, and M. Haataja, "Physical principles of intracellular organization via active and passive phase transitions," *Rep. Prog. Phys.*, vol. 80, p. 046601, April 2018.

[4] Y. Hanif and U. Saleem, "Coupled sine-Gordon systems in living cellular structure," *Mod. Phys. Lett. B*, vol. 34, p. 2050070, January 2020.

[5] A. J. Heeger, S. Kivelson, J. R. Schrieffer, and W. P. Su, "Solitons in conducting polymers," *Rev. Mod. Phys.*, vol. 60, pp. 781–850, July 1988.

[6] G. Kalosakas, A. V. Zolotaryuk, G. P. Tsironis, and E. N. Economou, "Propagation of solitons in hydrogen-bonded chains with mass variation," *Phys. Rev. E*, vol. 56, pp. 1088–1096, July 1997.

[7]V. A. Belinski and E. Verdaguer, *Gravitational Solitons*. Cambridge University Press, 2001. ISBN: 0-521-80586-4.

[8]G. A. Alekseev, "Collision of strong gravitational and electromagnetic waves in the expanding universe," *Phys. Rev. D*, vol. 93, p. 061501, March 2016.

[9]Y. I. Frenkel and T. Kontorova, "On the theory of plastic deformation and twinning," *J. Phys.*, vol. 1, pp. 137–149, 1939.

[10]P. Bak, "Commensurate phases, incommensurate phases and the devil's staircase," *Rep. Prog. Phys.*, vol. 45, pp. 587–629, 1982.

[11]T.-H. Kim, S. Cheon, and H. W. Yeom, "Switching chiral solitons for algebraic operation of topological quaternary digits," *Nat. Phys.*, vol. 13, pp. 444–447, May 2017.

[12]C. Yang, Q. Zhou, H. Triki, M. Mirzazadeh, M. Ekici, W.-J. Liu, A. Biswas, and M. Belic, "Bright soliton interactions in a (2+1)-dimensional fourth-order variable-coefficient nonlinear Schrodinger equation for the Heisenberg ferromagnetic spin chain," *Nonlinear Dyn.*, vol. 95, pp. 983–994, January 2019.

[13]C. T. Nelson, P. Gao, J. R. Jokisaari, C. Heikes, C. Adamo, A. Melville, S.-H. Baek, C. M. Folkman, B. Winchester, Y. Gu, Y. Liu, K. Zhang, E. Wang, J. Li, L.-Q. Chen, C.-B. Eom, D. G. Schlom, and X. Pan, "Domain dynamics during ferroelectric switching," *Science*, vol. 334, pp. 968–971, November 2011.

[14]S. Emori, U. Bauer, S.-M. Ahn, E. Martinez, and G. S. D. Beach, "Current-driven dynamics of chiral ferromagnetic domain walls," *Nat. Mater.*, vol. 12, pp. 611–616, July 2013.

[15]R. S. Elliott, N. Triantafyllidis, and J. A. Shaw, "Reversible stress-induced martensitic phase transformations in a bi-atomic crystal," *J. Mech. Phys. Solids*, vol. 59, pp. 216–236, February 2011.

[16]J. A. Shaw and S. Kyriakides, "Thermomechanical aspects of NiTi," *J. Mech. Phys. Solids*, vol. 43, pp. 1243–1281, August 1995.

[17]M. Mehboudi, B. M. Fregoso, Y. Yang, W. Zhu, A. van der Zande, J. Ferrer, L. Bellaiche, P. Kumar, and S. Barraza-Lopez, "Structural phase transition and material properties of few-layer monochalcogenides," *Phys. Rev. Lett.*, vol. 117, p. 246802, December 2016.

[18]C. M. Wayman and K. Otsuka, *Shape Memory Materials*. Cambridge University Press, 1998. ISBN: 0521663849.

[19]D. M. Kochmann and K. Bertoldi, "Exploiting microstructural instabilities in solids and structures: from metamaterials to structural transitions," *Appl. Mech. Rev.*, vol. 69, p. 050801, September 2017.

[20]D. Yang, L. Jin, R. V. Martinez, K. Bertoldi, G. M. Whitesides, and Z. Suo, "Phase-transforming and switchable metamaterials," *Extreme Mech. Lett.*, vol. 6, pp. 1–9, March 2016.

[21]N. Nadkarni, C. Daraio, R. Abeyaratne, and D. M. Kochmann, "Universal energy transport law for dissipative and diffusive phase transitions," *Phys. Rev. B*, vol. 93, p. 104109, March 2016.

[22]N. Nadkarni, A. F. Arrieta, C. Chong, D. M. Kochmann, and C. Daraio, "Unidirectional transition waves in bistable lattices," *Phys. Rev. Lett.*, vol. 116, p. 244501, June 2016.

[23]M. J. Frazier and D. M. Kochmann, "Atomimetic mechanical structures with nonlinear topological domain evolution kinetics," *Adv. Mater.*, p. 1605800, March 2017.

[24]M. Hwang and A. F. Arrieta, "Solitary waves in bistable lattices with stiffness grading: augmenting propagation control," *Phys. Rev. E*, vol. 98, p. 042205, October 2018.

[25]A. P. Browning, F. G. Woodhouse, and M. J. Simpson, "Reversible signal transmission in an active mechanical metamaterial," *Proc. R. Soc. A*, vol. 475, p. 20190146, July 2019.

[26]L. Jin, R. Khajehtourian, J. Mueller, A. Rafsanjani, V. Tournat, K. Bertoldi, and D. M. Kochmann, "Guided transition waves in multistable mechanical metamaterials," *Proc. Natl. Acad. Sci.*, vol. 17, pp. 2319–2325, January 2020.

[27]H. Yasuda, L. M. Korpas, and J. R. Raney, "Transition waves and formation of domain walls in multistable mechanical metamaterials," *Phys. Rev. Applied*, vol. 13, p. 054067, May 2020.

[28]A. Zareei, B. Deng, and K. Bertoldi, "Harnessing transition waves to realize deployable structures," *Proc. Natl. Acad. Sci.*, vol. 117, pp. 4015–4020, February 2020.

[29]P. J. Pascual and L. Vázquez, "Sine-Gordon solitons under weak stochastic perturbations," *Phys. Rev. B*, vol. 32, pp. 8305–8311, December 1985.

[30]P. Biller and F. Petruccione, "Dynamics of sine-Gordon solitons under random perturbations: Weak additive large-scale white noise," *Phys. Rev. B*, vol. 41, pp. 2139–2144, February 1990.

[31]J. A. González, A. Marcano, B. A. Mello, and L. Trujillo, "Controlled transport of solitons and bubbles using external perturbations," *Chaos, Solitons Fractals*, vol. 28, pp. 804–821, May 2006.

[32]M. T. Islam, X. S. Wang, and X. R. Wang, "Thermal gradient driven domain wall dynamics," *J. Phys.: Condens. Matter*, vol. 31, p. 455701, November 2019.

[33]D. Zhang, D. Sando, P. Sharma, X. Cheng, F. Ji, V. Govinden, M. Weyland, V. Nagarajan, and J. Seidel, "Superior polarization retention through engineered domain wall pinning," *Nat. Comm.*, vol. 11, p. 349, January 2020.

[34]T. Dauxois and M. Peyrard, *Physics of Solitons*. Cambridge University Press, 2006. ISBN: 0-521-85421-0.

[35]D. J. Bergman, E. Ben-Jacob, Y. Imry, and K.-i. Maki, "Sine-Gordon solitons: particles obeying relativistic dynamics," *Phys. Rev. A*, vol. 27, pp. 3345–3348, June 1983.

[36]N. Nadkarni, C. Daraio, and D. M. Kochmann, "Dynamics of periodic mechanical structures containing bistable elastic elements: From elastic to solitary wave propagation," *Physical Review E*, vol. 90, p. 023204, August 2014.

[37]M. J. Frazier and D. M. Kochmann, "Band gap transmission in periodic bistable mechanical systems," *J. Sound Vib.*, vol. 388, pp. 315–326, February 2017.

[38]V. Ramakrishnan and M. J. Frazier, "Multistable metamaterial on elastic foundation enables tunable morphology for elastic wave control," *J. Appl. Phys.*, vol. 127, p. 225104, June 2020.

[39]E. J. Markvicka, M. D. Bartlett, X. Huang, and C. Majidi, "An autonomously electrically self-healing liquid metal-elastomer composite for robust soft-matter robotics and electronics," *Nat. Mater.*, vol. 17, pp. 618–624, July 2018.

[40]C. Majidi, "Soft-matter engineering for soft robotics," *Adv. Mater. Technol. (Weinheim, Ger.)*, vol. 4, p. 1800477, February 2019.

[41]J. R. Raney, N. Nadkarni, C. Daraio, D. M. Kochmann, J. A. Lewis, and K. Bertoldi, "Stable propagation of mechanical signals in soft media using stored elastic energy," *Proc. Natl. Acad. Sci.*, vol. 113, pp. 9722–9727, 2016.